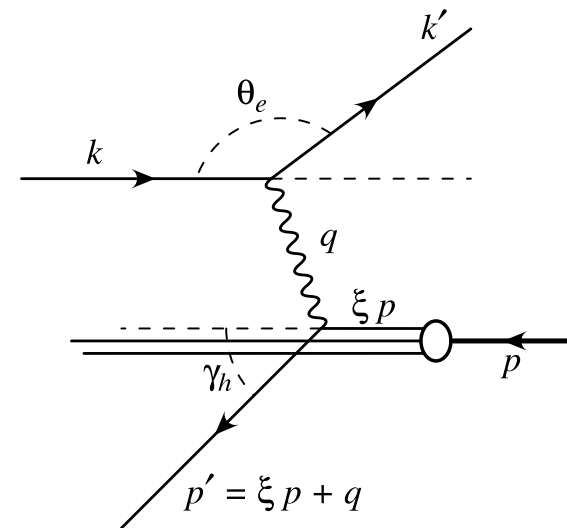


QCD Physics and HERA - Lecture IV

James Ferrando - ZEUS Collaboration.

11/2/2005.

- *QCD Introduction.*
- *HERA Accelerator.*
- *Experiments.*
- *Deep Inelastic Scattering.*
- *Proton Structure.*
- *Photon Structure.*
- *α_S measurements.*
- *Beyond the SM.*



Precision Measurements of α_S I

- *The strong coupling constant α_S is one of the fundamental parameters of QCD.*
- *The value of α_S is not predicted by the theory and must be determined by experiment.*
- *To obtain a high precision in this fundamental parameter, the combination of many measurements must be performed to reduce the uncertainties.*
- *Each measurement should be as precise as possible: selecting a phase-space region where the pQCD predictions are least affected by theoretical uncertainties permits a precise determination of α_S .*
- *At ZEUS, α_S has been measured in NC DIS using different methods:*
 - *Dijet cross sections in the Breit Frame at high Q^2 .*
 - *Inclusive jet cross sections in the Breit frame at high Q^2 .*
 - *Internal structure of jets: jet shape.*
 - *Internal structure of jets: subjet multiplicity.*
 - *An NLO QCD combined fit to inclusive NC DIS measurements (F_2) to obtain simultaneously the pPDFs and α_S .*
- *The independent methods give results consistent with each other and the world average.*

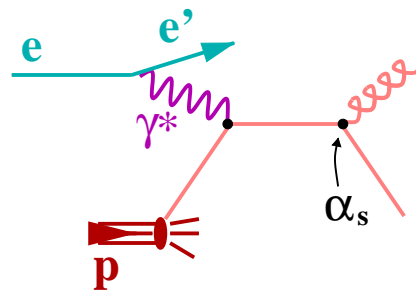
Precision Measurements of α_S II

- *The method to determine α_S is usually to make a measurement which is sensitive to its value and then perform a fit with α_S as the free parameter, using the best theoretical predictions available.*
- *In recent years, much progress on the development of process and observable independent algorithms that allow a complete and analytical cancellation of the soft and collinear singularities encountered in the calculation of the NLO cross sections.*
- *Flexible programs that compute arbitrary infrared and collinear-safe DIS observables in NLO QCD are now available (DISENT, MEPJET, DISASTER++, NLOJET).*
- *Restricting the measurements to a high- Q^2 kinematic region:*
 - *Avoids the large renormalisation-scale dependence of the NLO QCD dijet cross sections at lower Q^2 (20-50 % for $10 < Q^2 < 100 \text{ GeV}^2$)*
 - *Reduces the uncertainty due to the pPDFs (esp. gluon density).*
 - *Improves the reconstruction of the boost in the Breit frame.*
- *Using the asymmetric cuts on the transverse energy of the two jets avoids infrared sensitive regions where the behaviour of the cross section as predicted by the NLO QCD programs is unphysical.*

Dijet Cross Sections in the Breit Frame at high Q^2 I

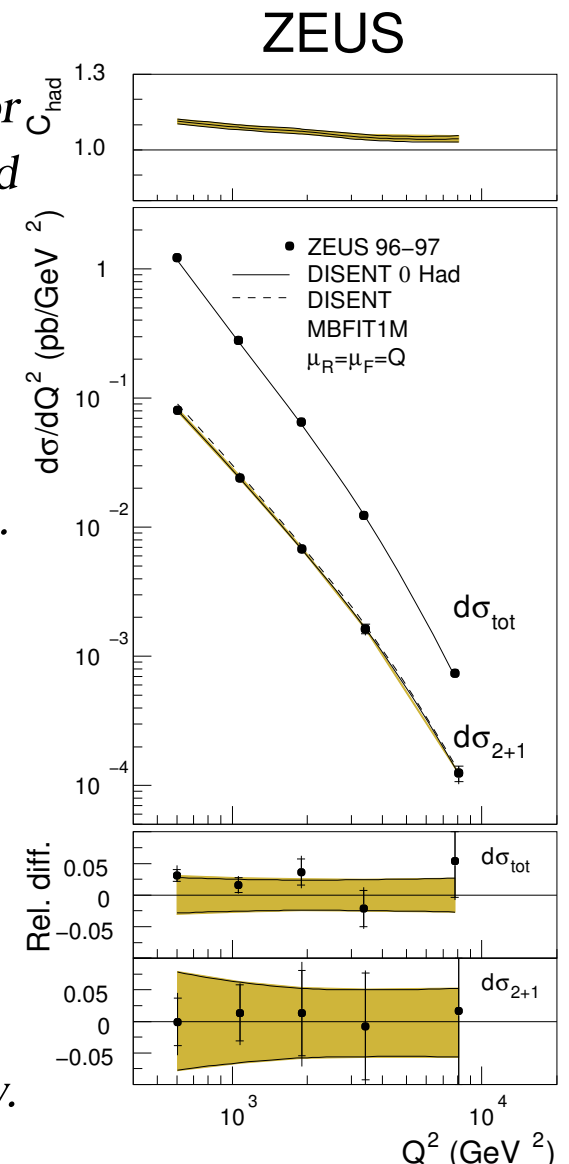
$$ep \rightarrow e + \text{jet} + \text{jet} \text{ (exclusive)}$$

- In the Breit frame the momentum transfer Q has vector $(0, 0, 0, Q)$, the struck quark enters with momentum $q/2$ and rebounds as though hitting a brick wall.
- Jets algorithm used: k_T cluster algorithm.
- $470 < Q^2 < 20000 \text{ GeV}^2$
- (2 jets) $E_{T,1}^{BRE} > 8 \text{ GeV}$, $E_{T,2}^{BRE} > 5 \text{ GeV}$, $-1 < \eta^{LAB}_{1,2} < 2$.



$$d\sigma_{ep \rightarrow e \text{ jet jet}} = \Sigma dx f(x, \alpha_S) d\sigma_{\gamma^* q \rightarrow qg}(x, \alpha_S)$$

- High Q^2 means experimental and theoretical errors are very low.
- Shape, magnitude of the measured σ described by NLO.

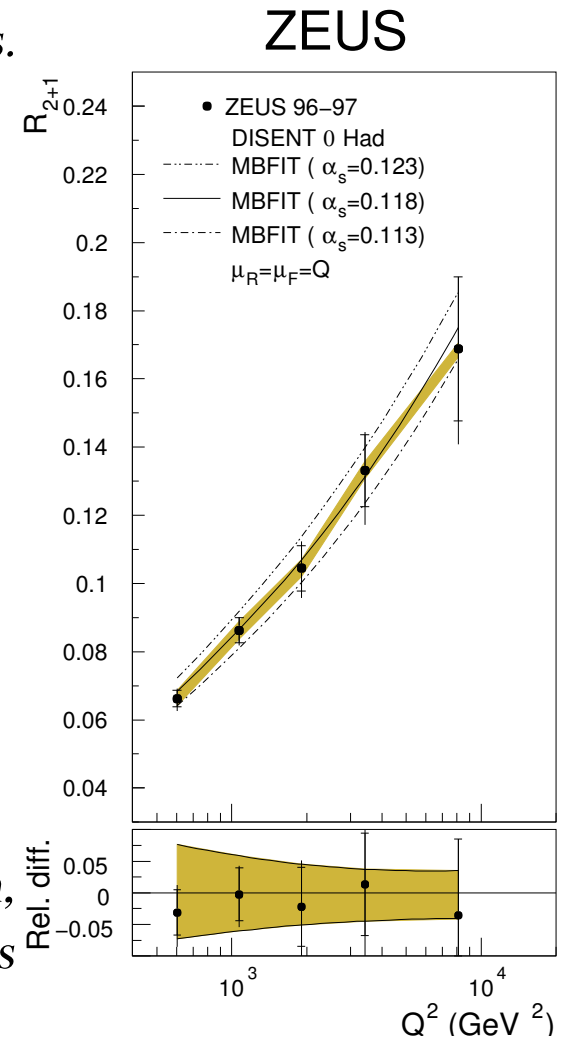


Dijet Cross Sections in the Breit Frame at High Q^2 II

- The extraction of α_S should be made from the ratios of the observables to reduce uncertainties and dependence on the PDFs.

$$\rightarrow \text{Ratio } R_{2+1} \equiv \frac{d\sigma_{2+1}/dQ^2}{d\sigma_{\text{tot}}/dQ^2}$$

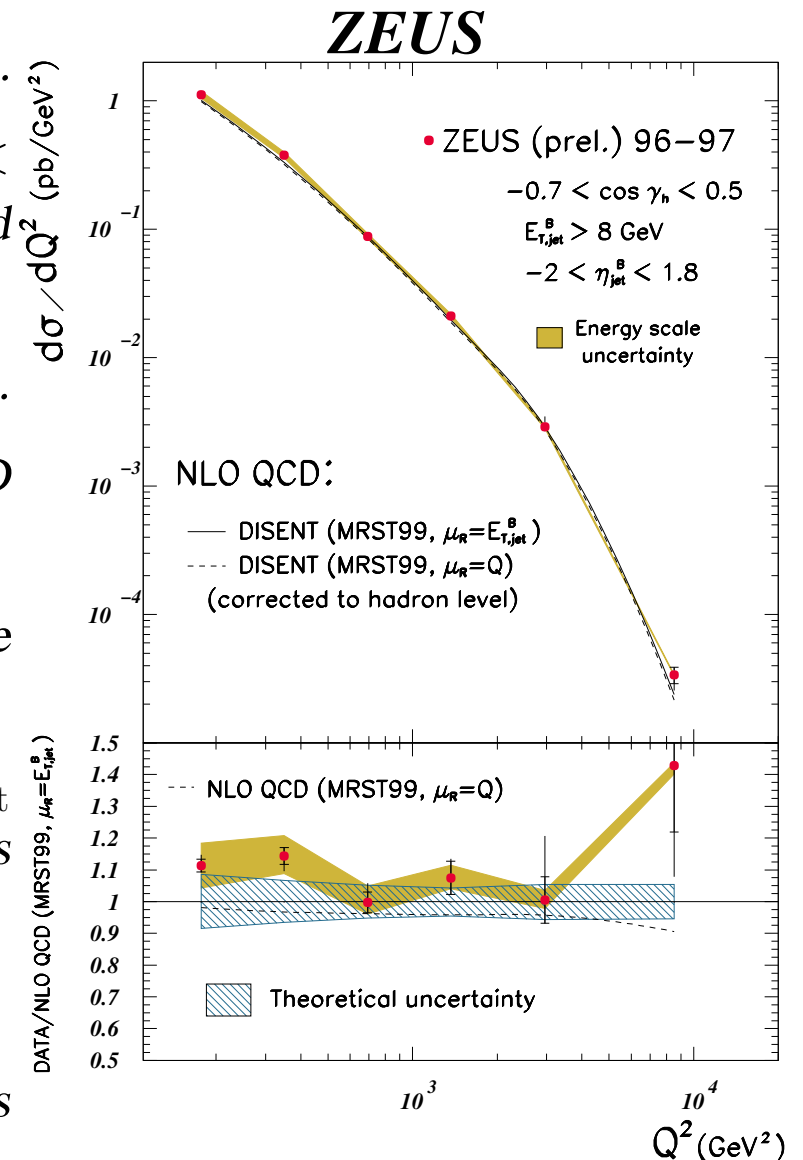
- Small experimental uncertainties.
- Small theoretical uncertainties:
 - Higher-order terms ($> NLO$) ($\sim 5\%$)
 - Value of α_S assumed ($\sim 6\%$)
 - Uncertainties on the proton PDFs ($\sim 1.5\%$)
 - Hadronisation corrections ($< 10\%$)
- Comparison with NLO QCD calculations:
 - the measured ratio is described by the prediction, demonstrating the validity of the description of the dynamics of dijet production by NLO QCD hard processes.



Inclusive Jet Cross Sections in the Breit Frame I

$$ep \rightarrow e + \text{jet} + X$$

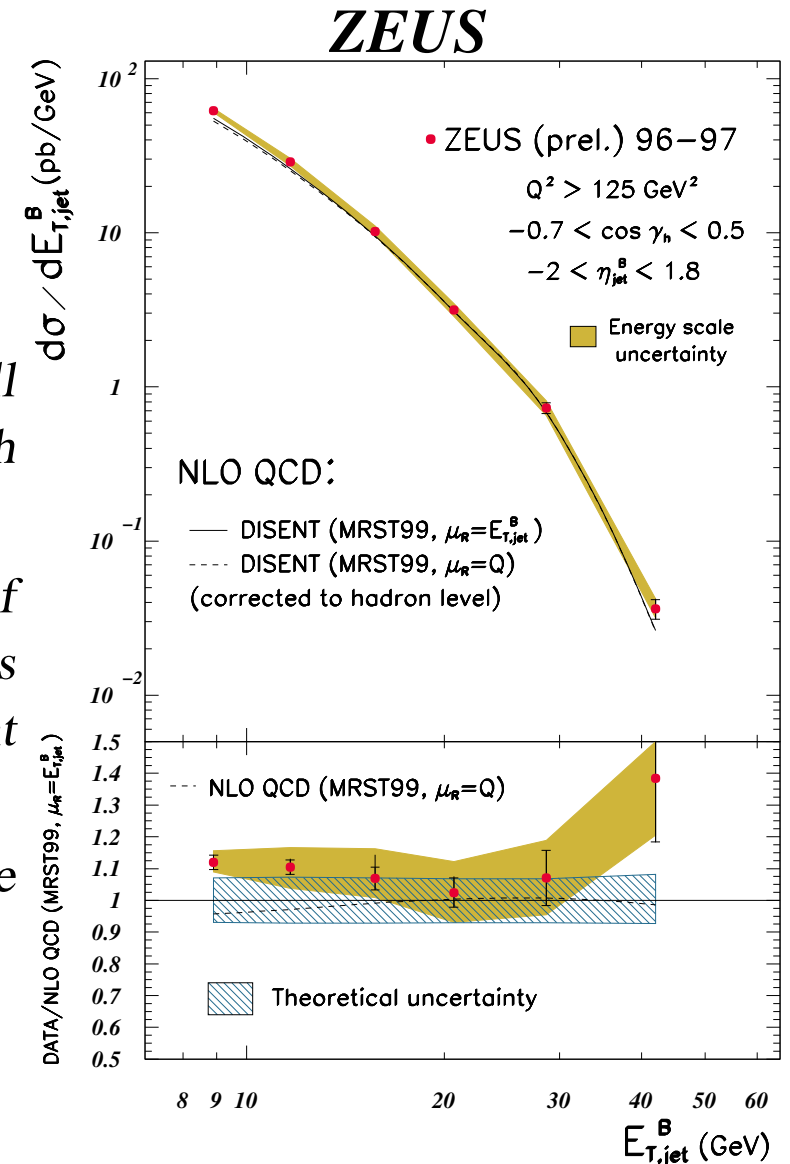
- Jets searched with k_T cluster algorithm in the Breit frame.
- Kinematic region $Q^2 > 125 \text{ GeV}^2$ and $-0.7 < \cos \theta < 0.5$ where γ corresponds to the direction of the scattered quark in the QPM.
- At least one jet with $E_{T,\text{jet}}^B > 8 \text{ GeV}$ and $-2\eta_{\text{jet}}^B < 1.8$.
- Advantages of inclusive jet cross sections in a QCD analysis:
 - Infrared insensitivity (calculation does not diverge when $E_g \rightarrow 0$)
 - For dijet cross section, assymmetric cuts on $E_{T,\text{jet}}^B$ are necessary to avoid the infrared-sensitive regions where NLO QCD programs are not reliable.
- Better to test resummed calculation.
- smaller theoretical uncertainties than in dijet cross sections.



Inclusive Jet Cross Sections in the Breit Frame II

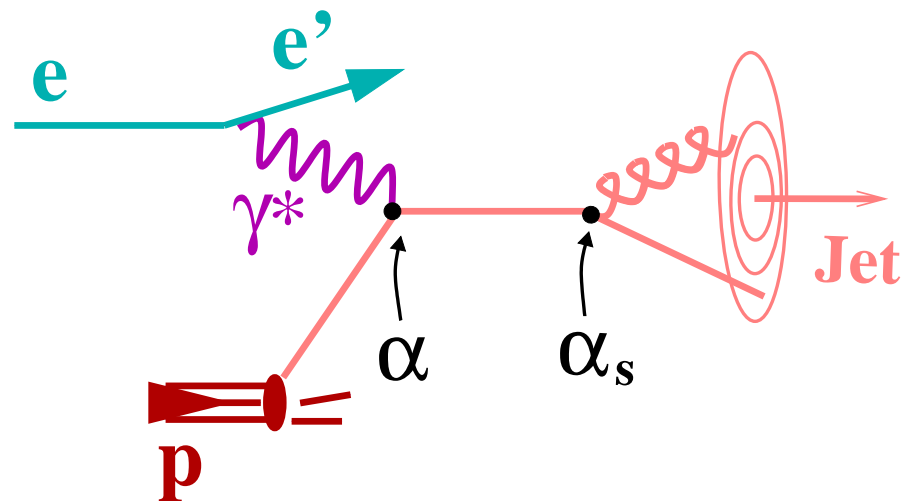
$$ep \rightarrow e + \text{jet} + X$$

- Comparison with NLO QCD calculations:
 - the measured inclusive jet cross sections are well described by the predictions at high Q^2 and at high $E_{T,\text{jet}}^B$.
 - At low Q^2 and at low $E_{T,\text{jet}}^B$, the measurements of inclusive jet cross sections are above the calculations by $\sim 12\%$ (origin of discrepancy at present unknown).
 - Therefore, the determination of α_S from these measurements is restricted to high scales.



Internal Jet Structure

- Internal jet structure presents an independent method for extracting α_S .
- This method exploits pQCD.
- The **Integrated Jet Shape** and **Mean Subject Multiplicity** in inclusive jet NC DIS which are calculable in pQCD at high E_T^{jet} .
- Dependence of calculations on knowledge of pPDFs reduced for this type of observable.
- Lowest non-trivial-order contribution to measurements from $\mathcal{O}(\alpha\alpha_S)$ pQCD calculations.
- Thus measurements of jet substructure provide a stringent test of pQCD calculations beyond LO and allow a determination of α_S by comparing NLO calculations of jet substructure to the measurements since in the LAB frame it is possible to have 3 partons inside one jet.



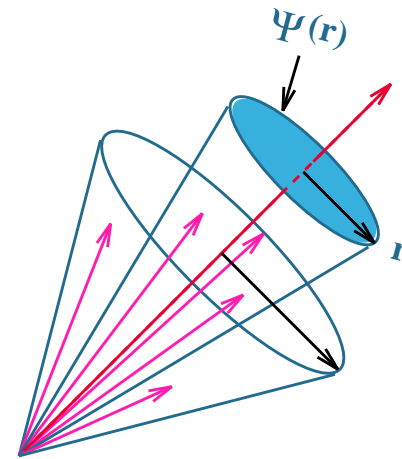
Internal Structure of Jets: Integrated Jet Shape

- The integrated jet shape is defined as the average fraction of the jet transverse energy that lies inside a cone in the $\eta - \phi$ plane of radius

$$r = \sqrt{(\Delta\eta)^2 + (\Delta\phi)^2}$$

concentric with the jet axis.

$$\langle \psi(r) \rangle = \frac{1}{N_{\text{jets}}} \sum_{\text{jets}} \frac{E_t(r)}{E_T^{\text{jets}}}$$



- In pQCD $\langle 1 - \psi(r) \rangle$ is calculated as the fraction of the jet's transverse energy due to parton emission that lies in the cone segment between r and $R = 1$.

$$\langle 1 - \psi(r) \rangle = \frac{\int dE_T E_T [d\sigma(ep \rightarrow 2\text{partons})/dE_T]}{E_T^{\text{jet}} \sigma_{\text{jet}}(E_T^{\text{jet}})}$$

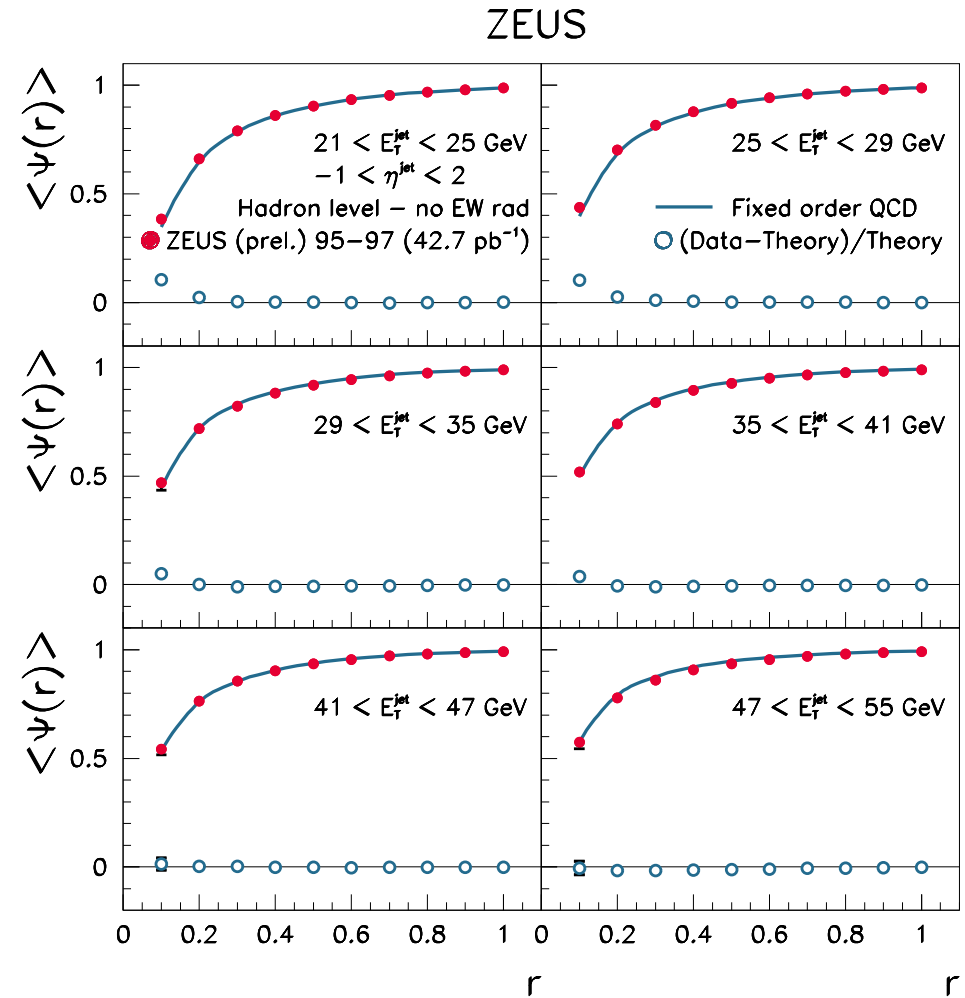
where $\sigma_{\text{jet}}(E_T^{\text{jet}})$ is the cross section for inclusive jet production.

- NLO QCD predictions for the integrated jet shape are derived from this formula by computing the numerator to $\mathcal{O}(\alpha\alpha_S^2)$ and denominator to $(\mathcal{O}(\alpha\alpha_S))$.

Internal Structure of Jets Integrated Jet Shape I

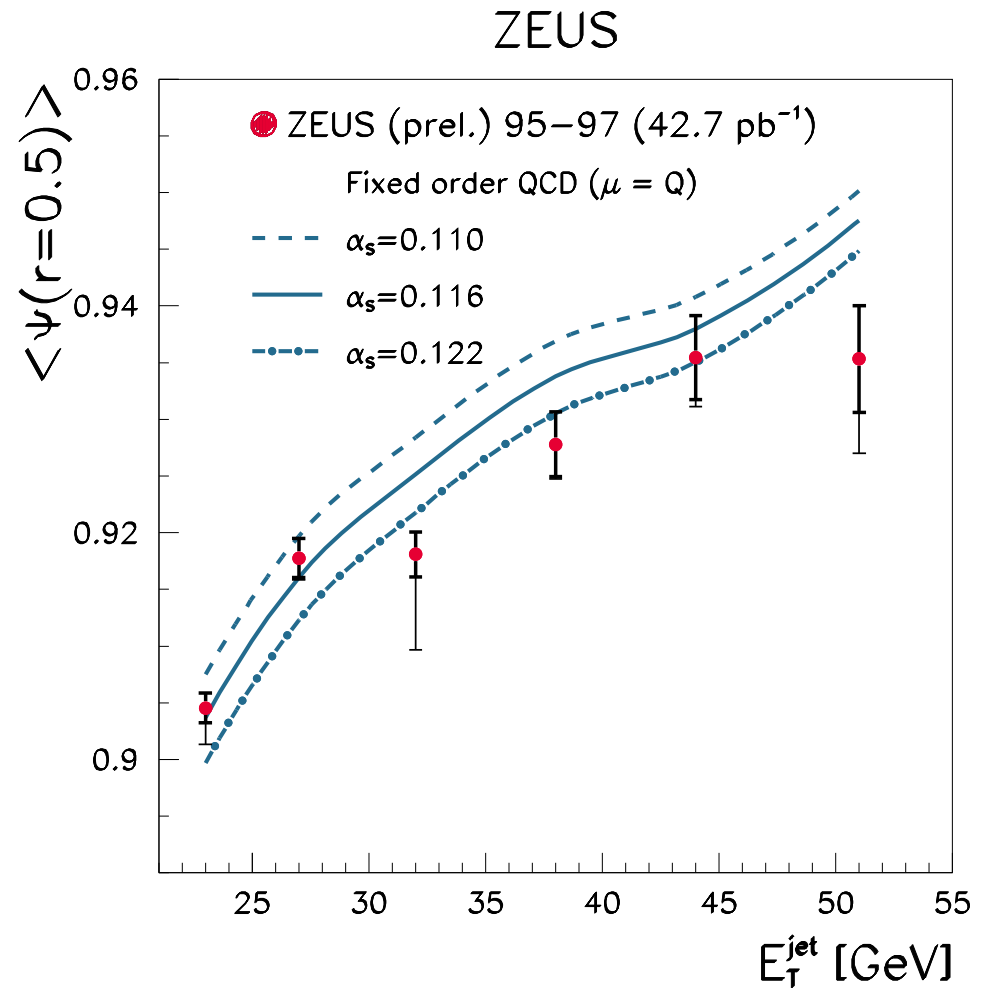
$$ep \rightarrow e + \text{jet} + X$$

- *Small experimental uncertainties for $r \geq 0.5$.*
 - *Fragmentation model dependence: $< 0.8\%$*
 - *Jet energy scale: $< 0.4\%$*
- *Small corrections s for $r \geq 0.5$.*
 - *Data (detector effects): $< 3\%$*
 - *NLO QCD calculations $< 5\%$*
- *Comparison with NLO QCD calculation:*
 - *Calculations provide a very good description of the data: $(\text{Data}-\text{NLO})/\text{NLO}$ smaller than 1.3 for $r = 0.5$.*



Internal Structure of Jets Integrated Jet Shape II

- The integrated jet shape at fixed values of r , $\langle \psi(r = 0.5) \rangle$, increases as E_T^{jet} increases: the jets become more collimated, as observed in $\gamma p \rightarrow$ effect of running of α_S .
 - These measurements are sensitive to the value of α_S
- The sensitivity of $\langle \psi(r = 0.5) \rangle$ as a function of E_T^{jet} to the value of $\alpha_S(M_Z)$ is seen by comparing the measurement to NLO QCD calculations using three different values of $\alpha_S(M_Z)$.
- Comparison with NLO QCD calculation:
 - Calculations provide a very good description of the data \rightarrow method can be used to determine $\alpha_S(M_Z)$.



The k_T Algorithm For Jet Finding.

The typical clustering algorithm used at ZEUS is the longitudinally invariant k_T clustering algorithm, used in the inclusive mode:

- For every pair of objects, a distance parameter d_{ij} is defined

$$d_{ij} = \min(E_{T,i}^2, E_{T,j}^2) R_{ij}^2 / R^2 \quad (1)$$

with the radius parameter R being of order unity, and R_{ij} the distance between the two objects in the $\eta - \phi$ plane $R_{ij}^2 = (\Delta\eta_{ij})^2 + (\Delta\phi_{ij})^2$.

- For every single object the distance parameter to the beam is defined as:

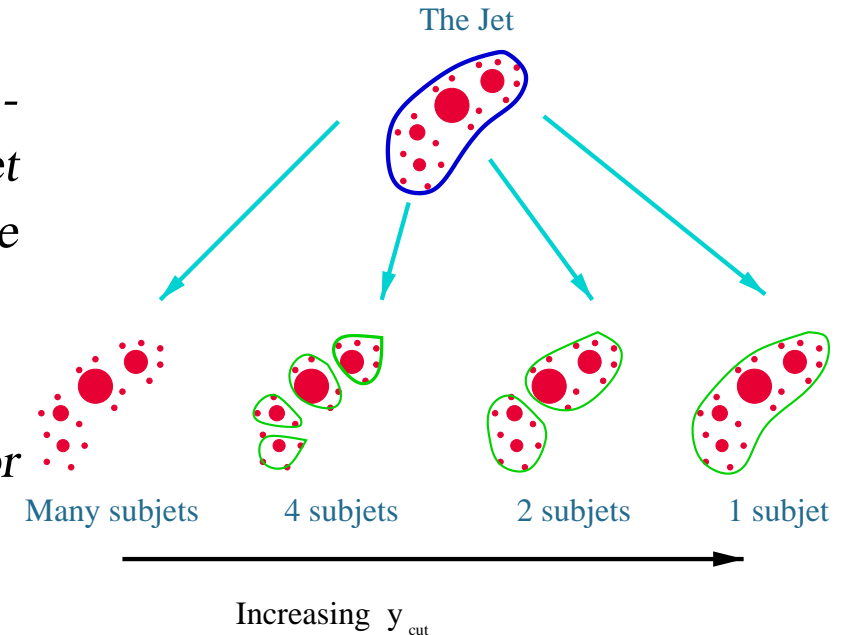
$$d_i = E_{T,i}^2. \quad (2)$$

- d_i and d_{ij} are compared; if d_{ij} is smaller than d_i then objects i and j are merged according to the Snowmass convention. Otherwise, the object is considered complete and removed from further clustering.
- The previous 3 steps are repeated on the remaining (combined) objects, until $d_i < d_{ij}, \forall i$

After the clustering, all jets below a chosen factorisation scale are considered as being factorised into the photon or proton beam remnants.

Internal structure of jets: subjet multiplicity I

- *Subjets are resolved within a jet by reapplying the k_T -cluster algorithm on all the particles belonging to the jet until, for every pair of particles the quantity d_{ij} is above $d_{\text{cut}} = y_{\text{cut}}(E_T^{\text{jet}})^2$.*
- *All remaining clusters are called subjets.*
- *The subjets structure depends upon the value chosen for the resolution parameter y_{cut} .*



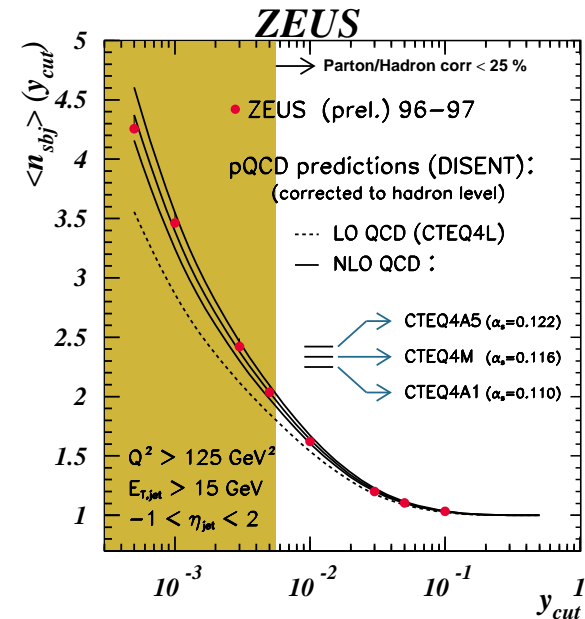
- *In pQCD the mean subjet multiplicity, $\langle n_{\text{subjet}} \rangle$ is calculated as the ratio of cross sections for $n_{\text{subjet}} - 1$ over that of inclusive jet production.*

$$\langle n_{\text{subjet}} \rangle = \frac{\sigma_{n_{\text{subjet}}-1}(E_T^{\text{jet}})}{\sigma_{\text{jet}}(E_T^{\text{jet}})} \approx \frac{A_{n_{\text{subjet}}-1} \cdot \alpha_S + B_{n_{\text{subjet}}-1} \cdot \alpha_S^2}{C_{\text{jet}} + D_{\text{jet}} \cdot \alpha_S} + \mathcal{O}(\alpha_S^3)$$

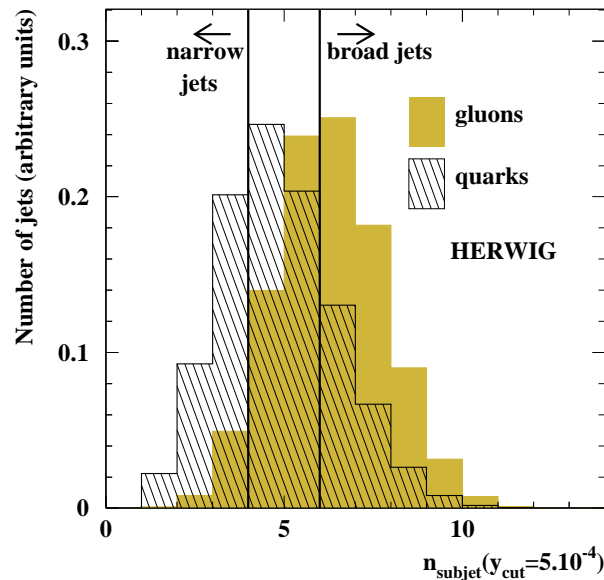
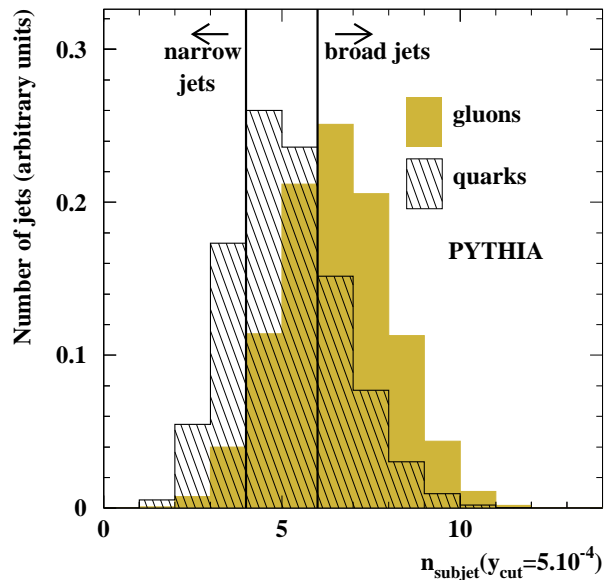
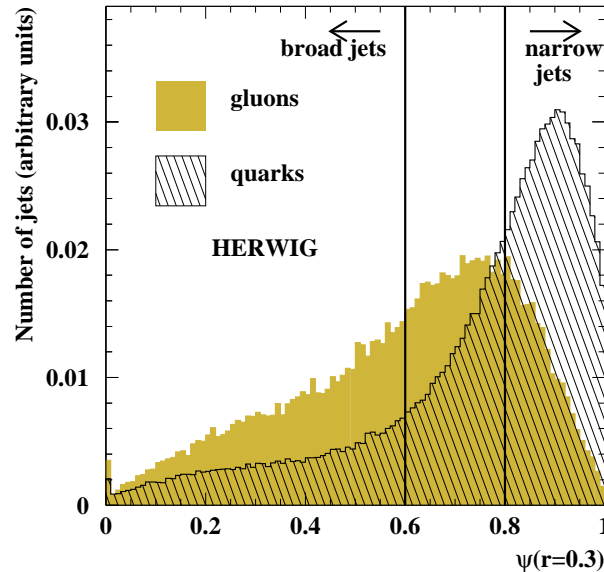
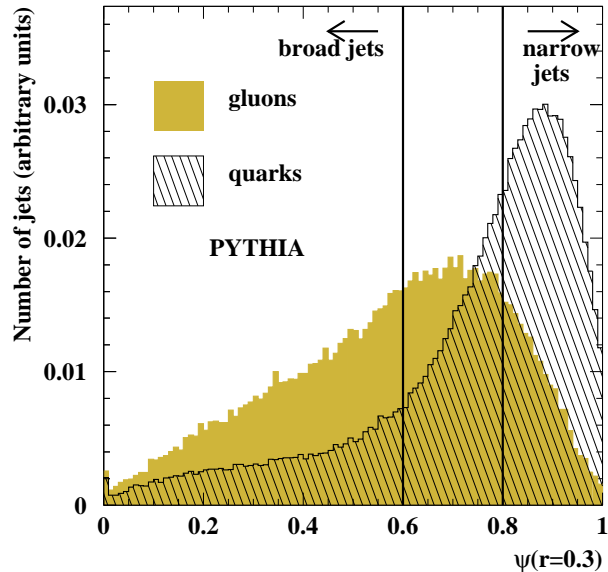
- *NLO QCD predictions for the mean subjet multiplicity are derived from this formula by adding 1 and computing the numerator to $\mathcal{O}(\alpha\alpha_S^2)$ and the denominator to $\mathcal{O}(\alpha\alpha_S)$.*

Internal structure of jets: subjet multiplicity II

- *Theoretical advantages of $\langle n_{\text{subjet}} \rangle$*
 - “safe” observables definable at any order in pQCD
 - useful tool to investigate colour dynamics.
 - small hadronisation corrections
- *All remaining clusters are called subjets.*
- *The subjets structure depends upon the value chosen for the resolution parameter y_{cut} .*
- *Small uncertainties for $y_{\text{cut}} \geq 0.01$*
 - *Fragmentation model dependence: $< 3\%$ jet energy scale: $\sim 1\%$*
- *Small corrections for $y_{\text{cut}} \geq 0.01$*
 - *(Detector effects): $< 10\%$ NLO(parton-hadron effects): $< 15\%$ for $E_T^{\text{jet}} > 25 \text{ GeV}$.*
- *Comparison with QCD calculations:*
 - *the LO calculations fail to describe the data.*
 - *NLO calculations provide a good description.*

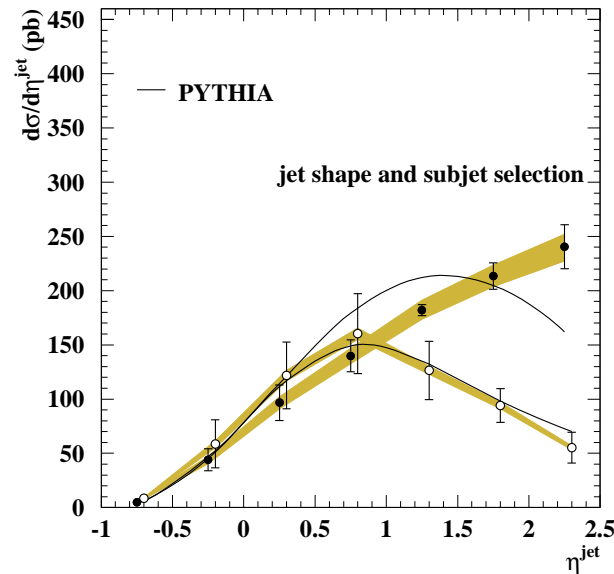
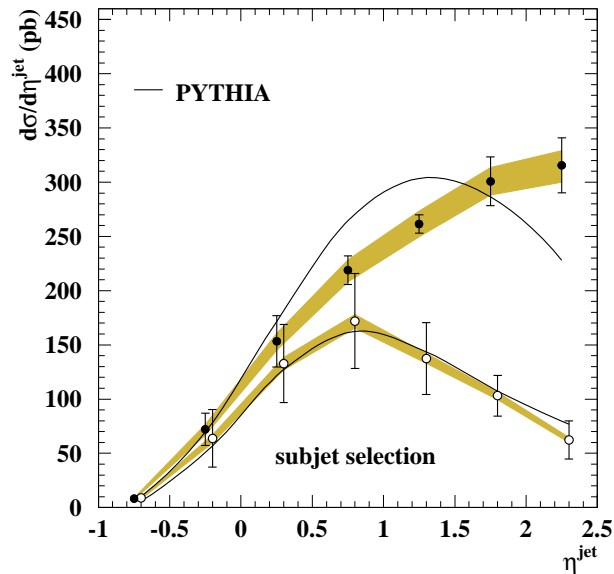
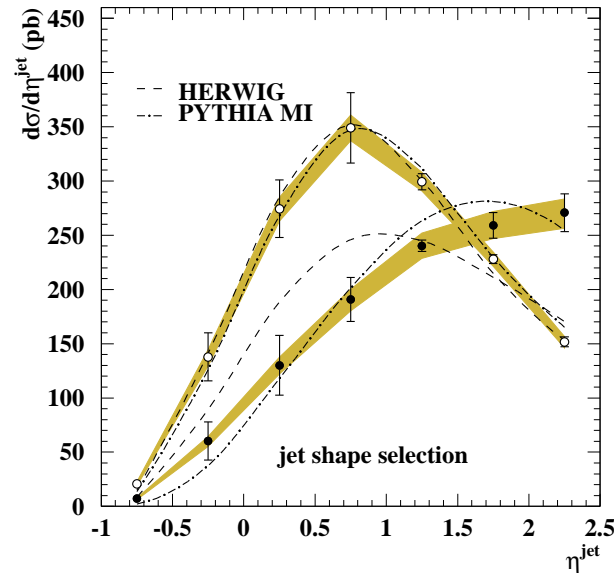
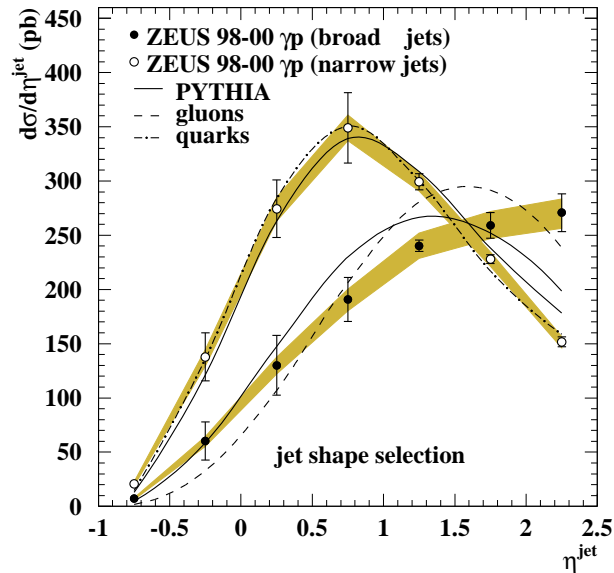


Internal Structure: Separating Quark Jets from Gluon Jets I



- *Gluon jets should be broader than Quark jets.*
- *$\psi(r = 0.3)$ peaks at lower values for gluons than for quarks.*
- *$n_{\text{subjet}}(y_{\text{cut}} = 5.10^{-4})$ peaks at higher values for gluons than for quarks.*

Internal Structure: Separating Quark Jets from Gluon Jets II



- Quark and gluon MC normalised to data cross sections describe narrow and broad jets respectively.

α_S from Dijet Cross Sections I

- The procedure to determine $\alpha_S(M_Z)$ from the dijet fraction as a function of Q^2 , $R_{2+1}(Q^2)$ was:
 - NLO calculations were performed using three sets of the *MBFIT* pPDFs and the value of $\alpha_S(M_Z)$ assumed in each calculation is that of the PDF set.
 - These were used to parameterise the $\alpha_S(M_Z)$ dependence of $R_{2+1}(Q^2)$, according to:
$$R_2^i(\alpha_S(M_Z)) = A_1^i \alpha_S(M_Z) + A_2^i \alpha_S^2(M_Z)$$
 - The value of α_S was then determined by a χ^2 fit to the parameterisation of the measured values.
- this procedure correctly handles the complete α_S dependence on the NLO cross sections (explicit dependence on partonic σ implicit from pPDFs) and preserves the correlation between α_S and the PDFs.

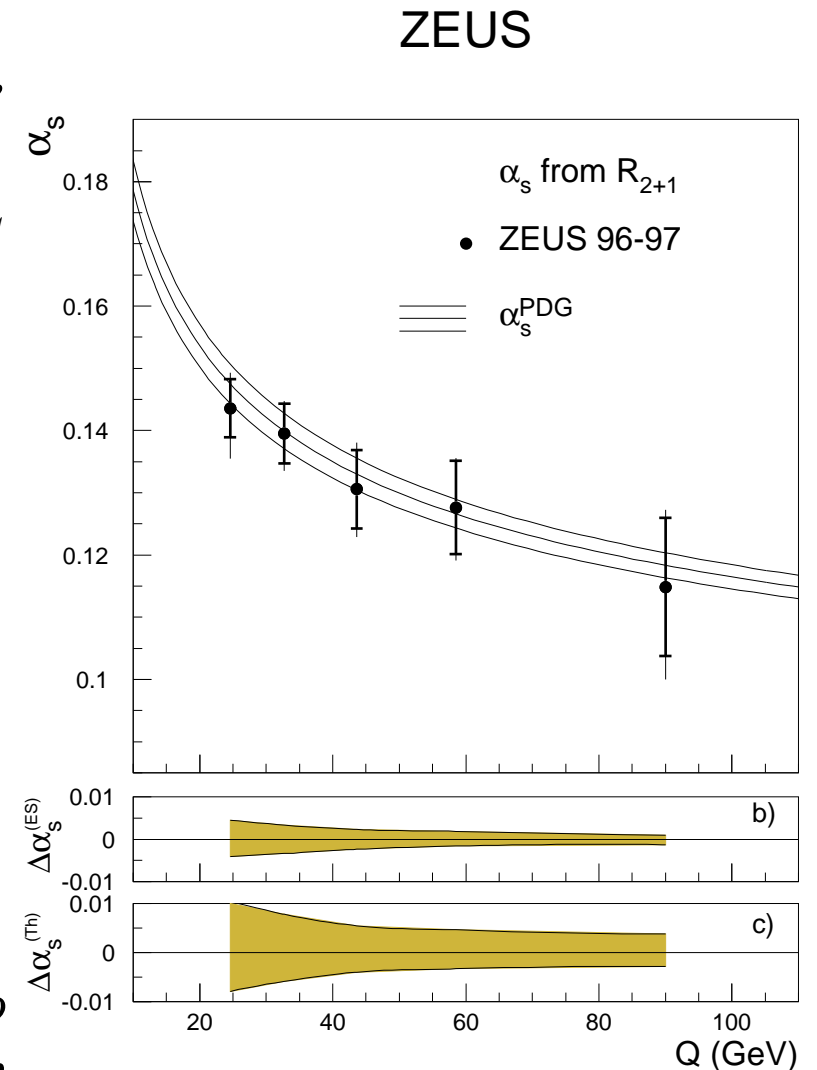
α_S from Dijet Cross Sections II

- Study the scale dependence of $\alpha_S(Q)$:
 - From the measured $R_{2+1}(Q^2)$ in each Q^2 region, α_S is extracted.
 - Measurements are consistent with running of α_S as predicted by QCD.
- A combined value of α_S has been extracted:

$$\alpha_S(M_Z) = 0.1166 \pm 0.0019(\text{stat.}) \begin{matrix} +0.0033 \\ -0.0024 \end{matrix} (\text{exp.})$$

$$\begin{matrix} +0.0044 \\ -0.0057 \end{matrix} (\text{th.})$$

- the theoretical uncertainties dominate:
 - Terms beyond NLO.
 - Uncertainties from pPDFs
 - Hadronisation corrections
 - Need improvement in theoretical calculations to obtain a more precise determination of α_S from the dijet cross section at high Q^2 .



α_S from Inclusive Jet Cross Sections

- Similar method to dijet measurement:
 - Differential cross sections are used not dijet fraction.
 - Different values obtained.
- $d\sigma/dQ^2, Q^2 > 125 \text{ GeV}^2$.

$$\alpha_S(M_Z) = 0.1241 \pm 0.0009(\text{stat.}) \begin{matrix} +0.0038 \\ -0.0043 \end{matrix}(\text{exp.}) \begin{matrix} +0.0036 \\ -0.0052 \end{matrix}(\text{th.})$$

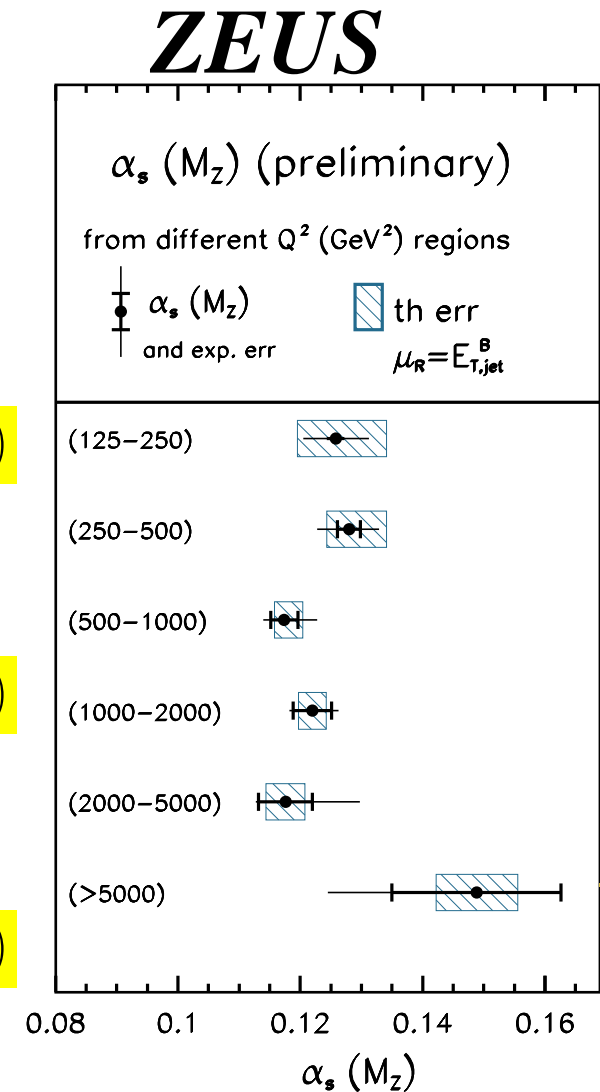
- $d\sigma/dQ^2, Q^2 > 500 \text{ GeV}^2$.

$$\alpha_S(M_Z) = 0.1190 \pm 0.0017(\text{stat.}) \begin{matrix} +0.0023 \\ -0.0049 \end{matrix}(\text{exp.}) \begin{matrix} +0.0026 \\ -0.0028 \end{matrix}(\text{th.})$$

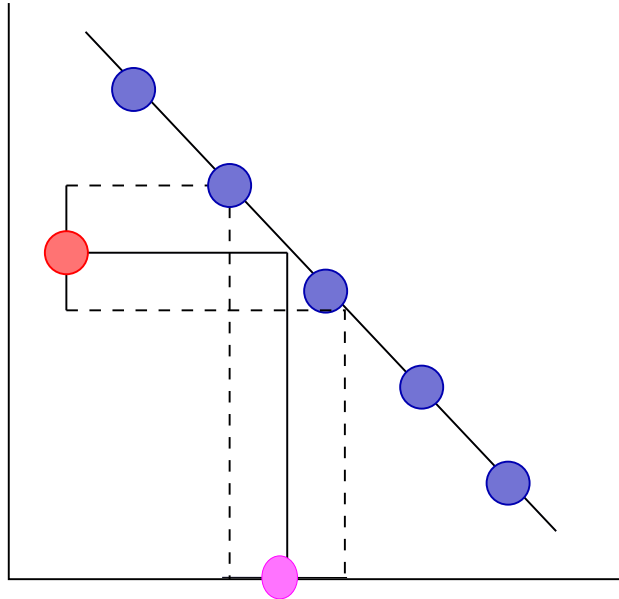
- $d\sigma/dE_T^{\text{jet}}, E_T^{\text{jet}} > 14 \text{ GeV}$.

$$\alpha_S(M_Z) = 0.1206 \pm 0.0015(\text{stat.}) \begin{matrix} +0.0045 \\ -0.0058 \end{matrix}(\text{exp.}) \begin{matrix} +0.0039 \\ -0.0041 \end{matrix}(\text{th.})$$

- Need improvement in theoretical calculations to obtain a more precise determination of α_S from inclusive cross sections.



Method to Determine α_S from the Internal Structure of Jets



- Procedure to determine $\alpha_S(M_Z)$ from the measured $\langle \psi(r = 0.5) \rangle$ for $E_T^{\text{jet}} > 21 \text{ GeV}$ and $\langle n_{\text{subject}} \rangle$ at $y_{\text{cut}} = 0.01$ for $E_T^{\text{jet}} > 25 \text{ GeV}$ is the same as before.
 - NLO calculations were performed using five sets of CTEQ4 pPDFS and the value of $\alpha_S(M_Z)$ assumed in each calculation is that of each PDF set.
 - Calculations are used to parametrise the $\alpha_S(M_Z)$ dependence of $V(\langle \psi(r = 0.5) \rangle)$, $\langle n_{\text{subject}} \rangle$ at $y_{\text{cut}} = 0.01$
- The value of $\alpha_S(M_Z)$ was then determined by a χ^2 fit of the parameterisation of the measured values.
- This procedure correctly handles the complete α_S dependence on the NLO cross sections (explicit from dependence on partonic σ implicit from pPDFs) and preserves the correlation between α_S and the PDFs.

α_S the Internal Structure of Jets

- From the measured $\langle \psi(r = 0.5) \rangle$ and $\langle n_{\text{subject}} \rangle$ at $y_{\text{cut}} = 0.01$ in each E_T^{jet} region a value of α_S has been extracted from each observable.

– ψ

$$\alpha_S(M_Z) = 0.1179 \pm 0.0014(\text{stat.}) \begin{matrix} +0.0065 \\ -0.0054 \end{matrix}(\text{exp.}) \begin{matrix} +0.0073 \\ -0.0094 \end{matrix}(\text{th.})$$

– n_{subject}

$$\alpha_S(M_Z) = 0.1185 \pm 0.0016(\text{stat.}) \begin{matrix} +0.0048 \\ -0.0067 \end{matrix}(\text{exp.}) \begin{matrix} +0.0071 \\ -0.0089 \end{matrix}(\text{th.})$$

- The theoretical uncertainties dominate:
 - Terms beyond NLO
 - Hadronisation corrections.
 - Need improvement in theoretical calculations to obtain a more precise determination of α_S from the internal structure of jets.

NLO fit to determine α_S and proton PDFs I

- *NLO DGLAP equations were used to fit simultaneously the high precision ZEUS data on NC e^+p DIS and fixed target data at larger x to obtain the pPDFs.*
- *Fixed-target data were used to gain information on the valence distributions and the flavour composition of the sea, and to constrain the fit at high x (BCDMS,NMC,E665,CCFR)*
- *The precision ZEUS data provide information on the gluon and quark densities at low x .*
- *The kinematic range covered by the data input to the fits is:*

$$6.3 \times 10^{-5} \leq x \leq 0.65 \text{ and } 2.5 \leq Q^2 \leq 30000 \text{ GeV}^2$$

- *The fits have been performed within the framework of the NLO DGLAP evolution equations.*
- *These equations yield the quark and gluon momentum distributions at all values of Q^2 provided they are input as functions of x at some scale Q_0^2 ; the input scale was chosen to be $Q_0^2 = 7 \text{ GeV}^2$.*

NLO fit to determine α_S and proton PDFs II

- The PDFs were parameterised at $Q_0^2 = 7 \text{ GeV}^2$ by the form:

$$p_1 x^{p_2} (1-x)^{p_3} (1 + p_4 \sqrt{x} + p_5 x)$$

so that the distributions are either 0 or singular as $x \rightarrow 0$, and tend to 0 as $x \rightarrow 1$

- The parton momentum distributions that were parameterised are:

$$u \text{ valence: } x u_v = x(u - \bar{u})$$

$$d \text{ valence } x d_v = x(d - \bar{d})$$

$$\text{total sea: } x S = 2x(\bar{d} + \bar{u} + \bar{s} + \bar{c})$$

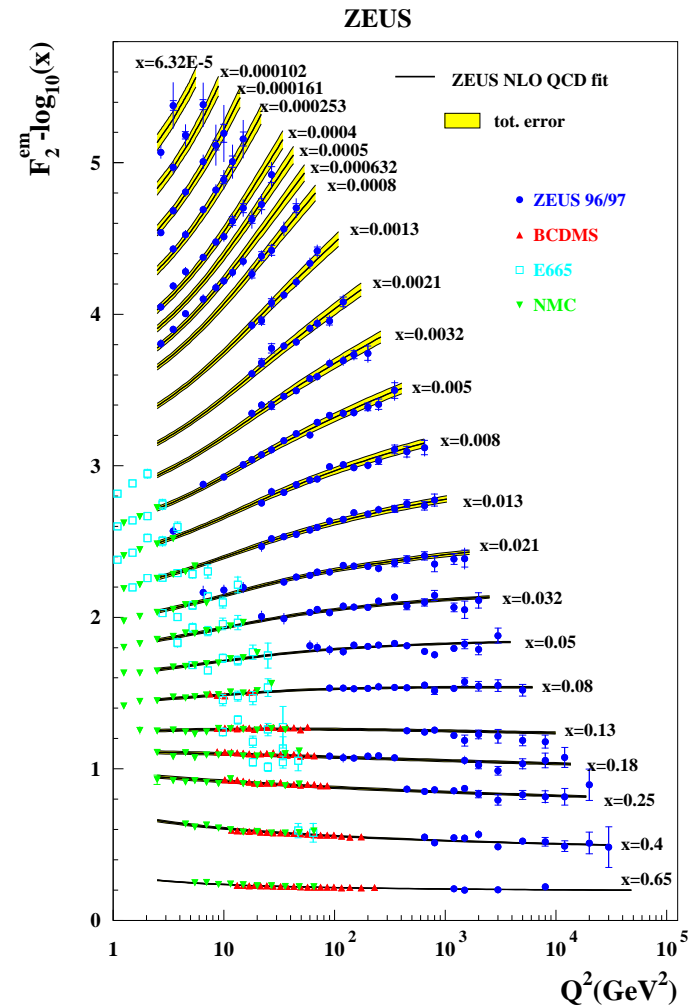
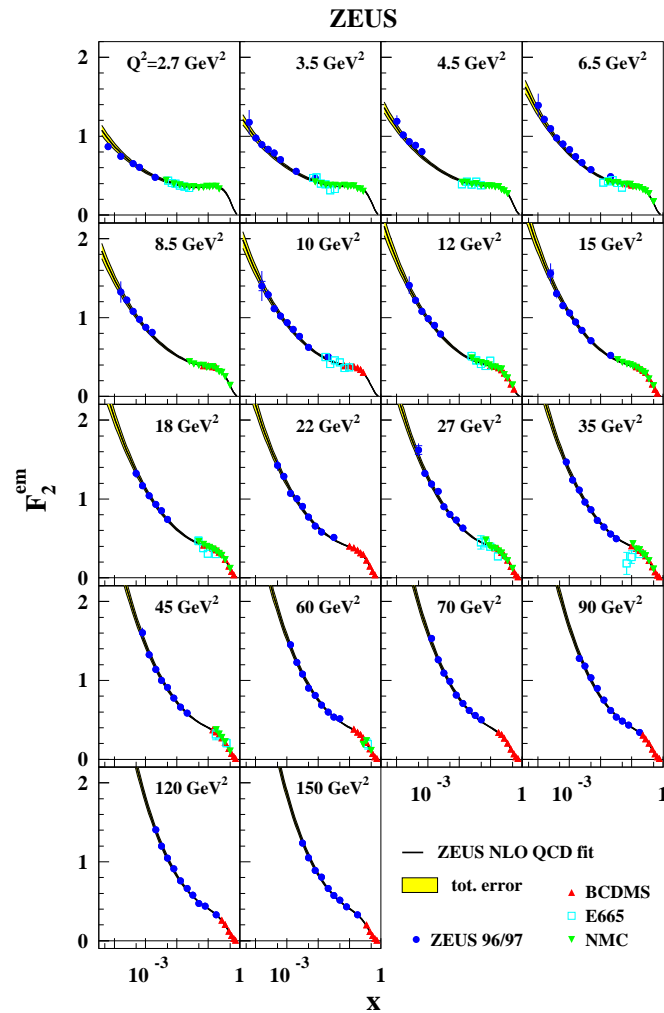
$$\text{gluon: } x g \text{ difference between } d \text{ and } u \text{ sea contribution: } x \Delta \equiv x(\bar{d} - \bar{u})$$

- Impose number and momentum sum rules:

$$\int_0^1 (xg + x\Sigma) dx = 1; \int_0^1 d_v dx = 1; \int_0^1 u_v dx = 2$$

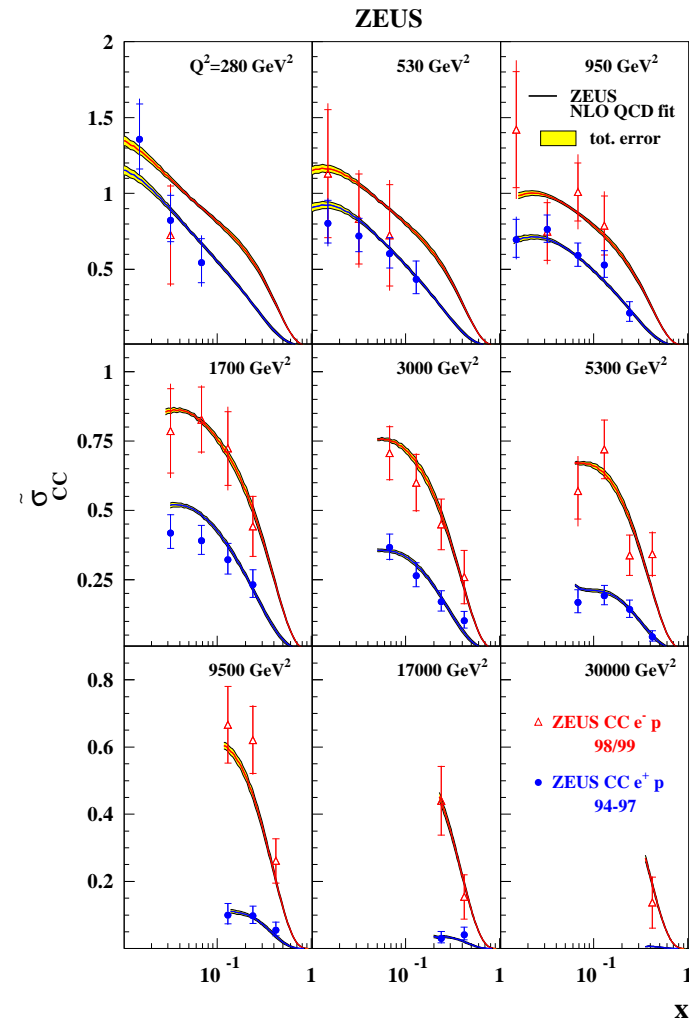
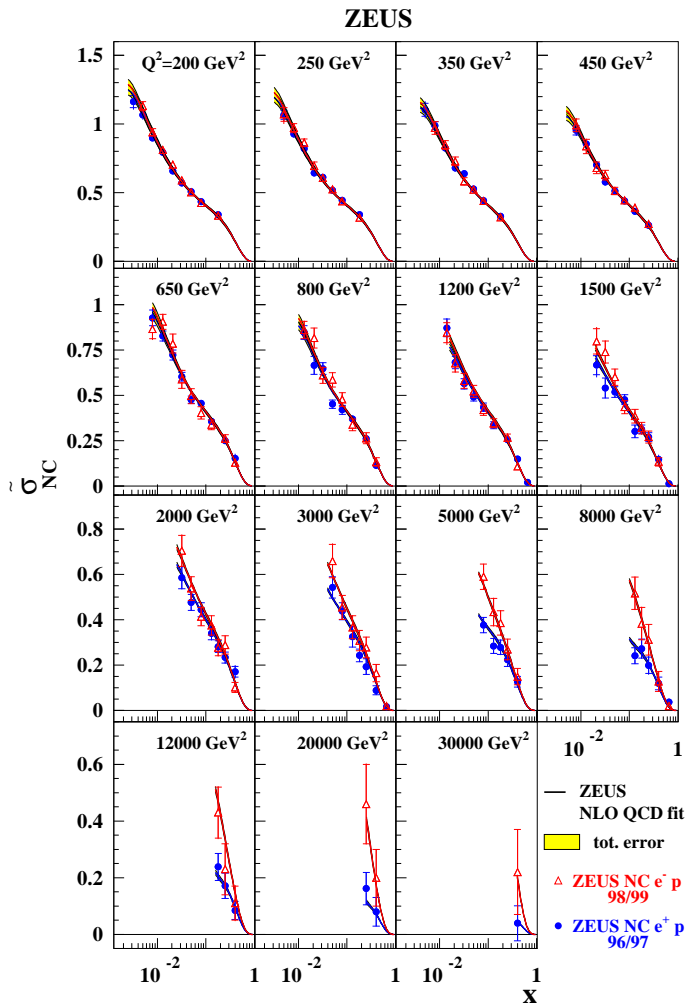
$$(x\Sigma = xS + x u_v + x d_v)$$

Results of NLO Fit: F_2 I



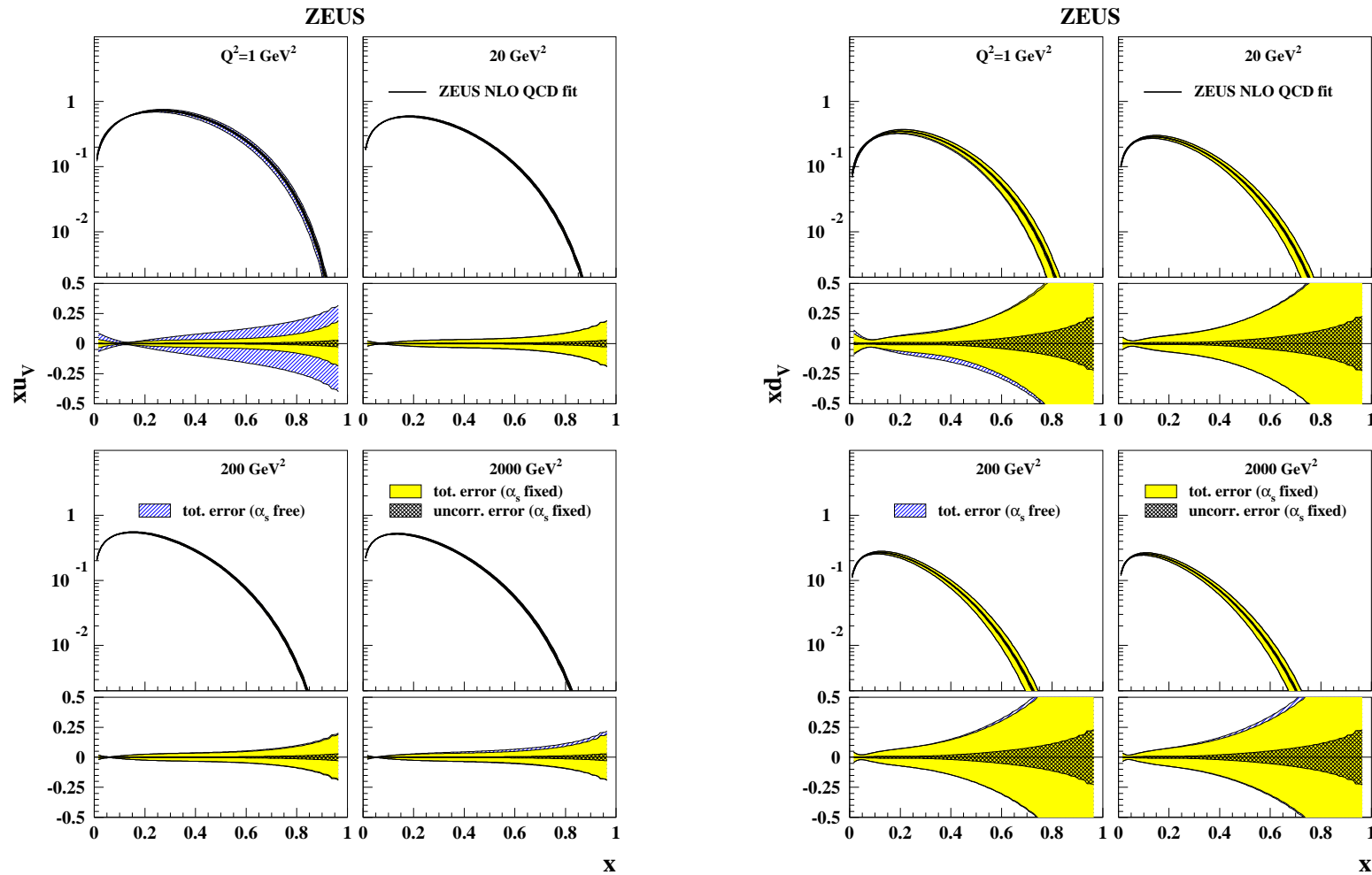
An excellent description of high precision ZEUS and fixed-target data.

Results of NLO Fit: F_2 II



A good description of high Q^2 data not used in the fit is achieved.

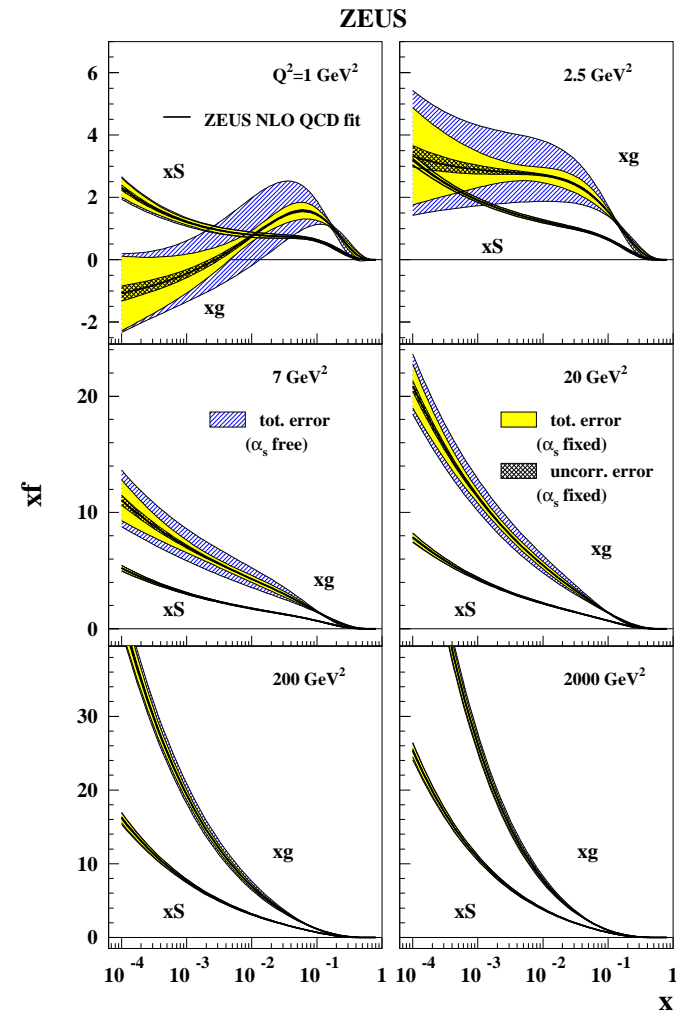
Results of NLO Fit: F_2 III



u-valence is much better determined (more *u* quark information from fixed target data)

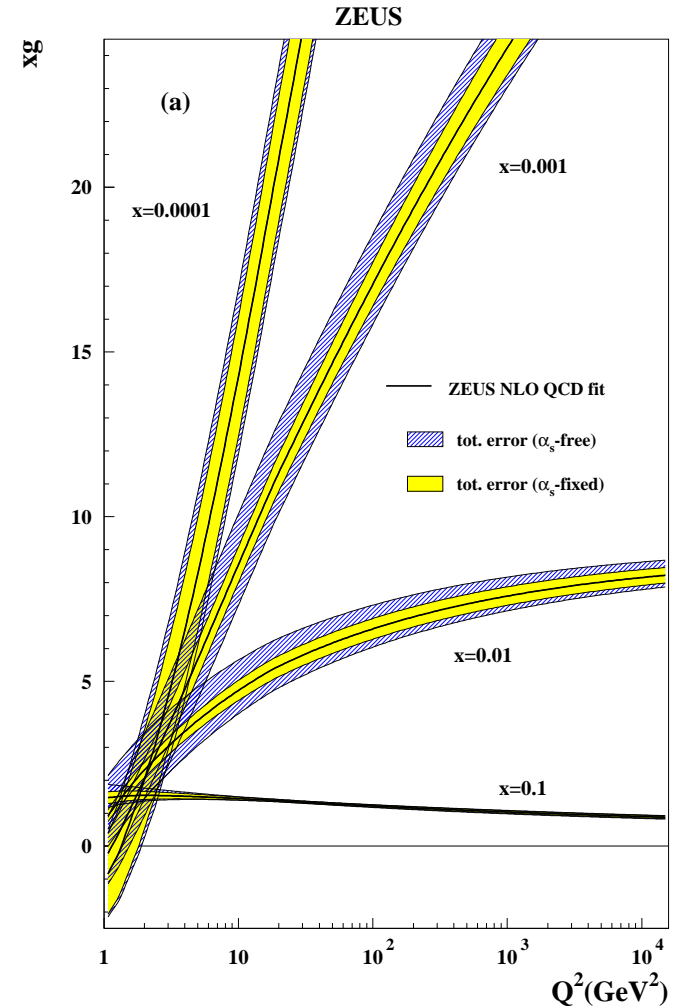
Results of NLO Fit: F_2 IV

- *Extracted sea and gluon distributions as a function of x for different Q^2 values.*
- *The uncertainty in the sea distribution of less than $\sim 5\%$ for $Q^2 \geq 2.5 \text{ GeV}^2$ and $10^{-4} < x < 10^{-1}$.*
- *The gluon distribution is determined to within $\sim 10\%$ for $Q^2 \geq 5 \text{ GeV}^2$ and $10^{-4} < x < 10^{-1}$.*
- *The sea distribution rises at small x .*
- *For $Q^2 \geq 5 \text{ GeV}^2$, the gluon becomes much larger than the sea but for lower x where the sea continues to rise, the gluon is suppressed.*



Results of NLO Fit: F_2 V

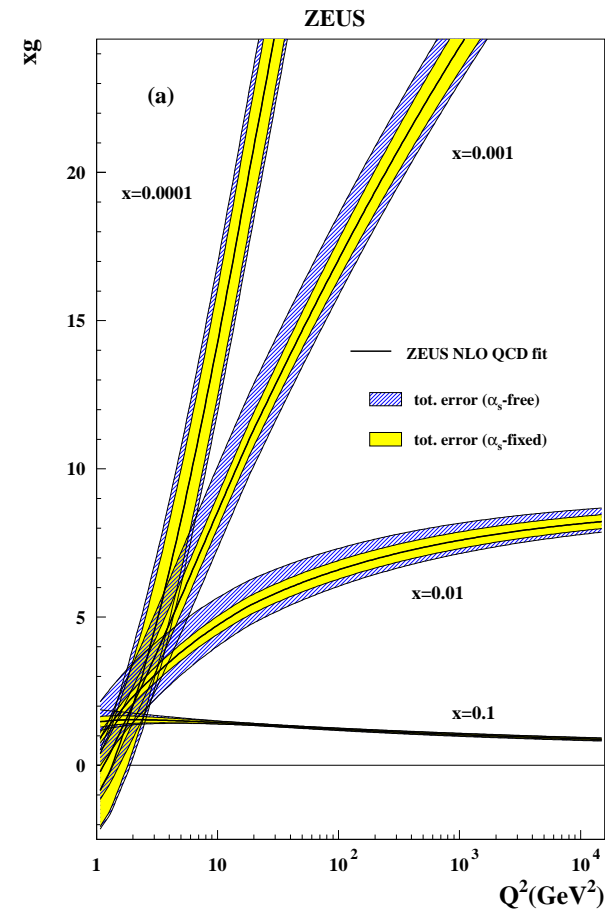
- Extracted gluon distributions as a function of Q^2 for different x values.
- Scaling violations of the gluon distribution can be clearly seen.
- Tendency of gluon to become negative at low x and low Q^2 indicates that pQCD could be inadequate for describing this regime. (scale too low)



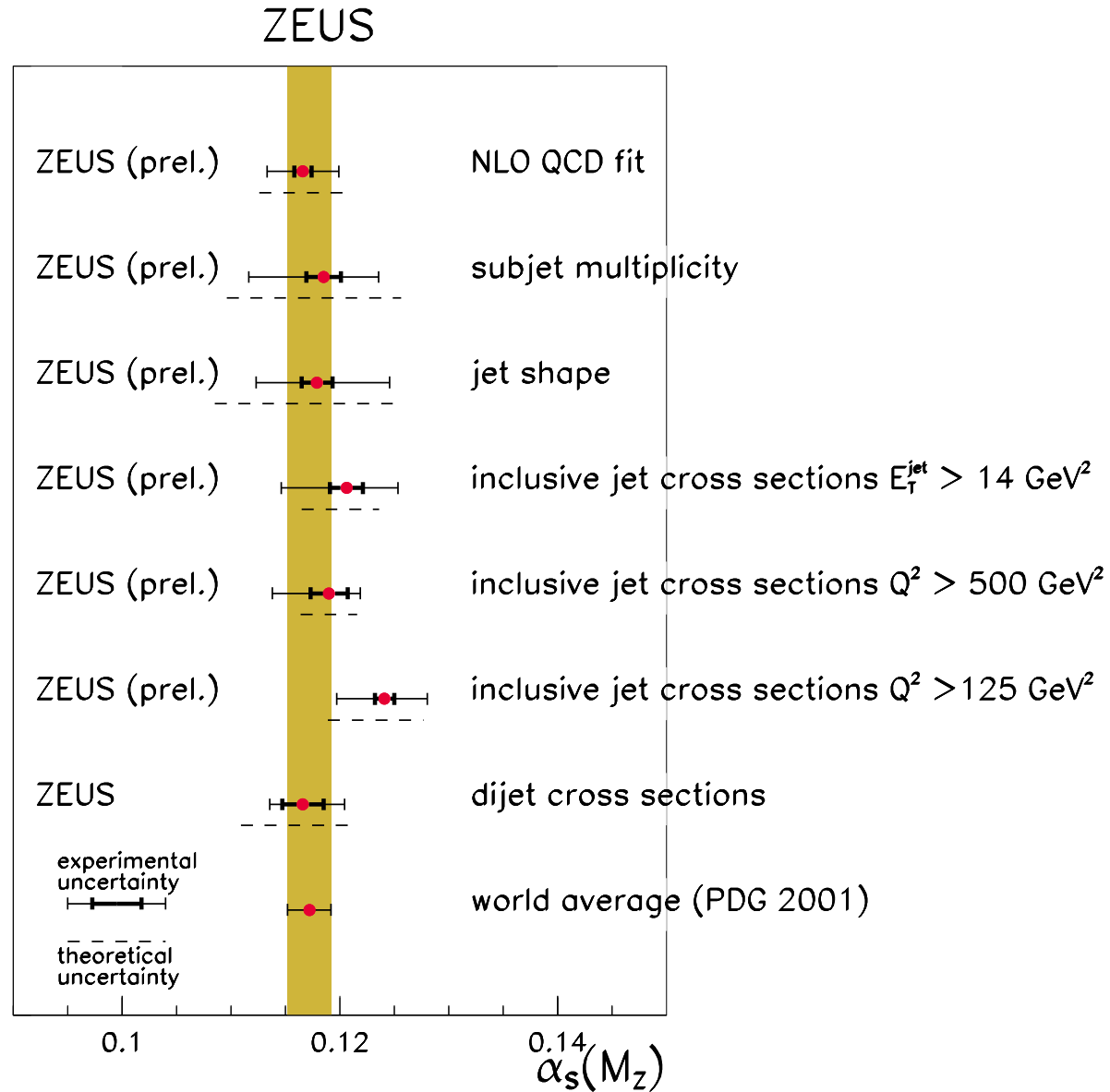
Method to determine α_S from a simultaneously NLO fit

- In the evolution of singlet quark distributions at intermediate x ($0.01 < x < 0.3$), the value of $\alpha_S(M_Z)$ and the gluon density are strongly correlated through the DGLAP equations and an increase in $\alpha_S(M_Z)$ can be compensated by a harder gluon distribution.
- At small x ($x < 0.01$) this correlation is weakened, since the gluon then drives the behaviour of F_2 as well as that of $dF_2/d\ln(Q^2)$
- Thus precision low- x data can be used to make a simultaneous fit of $\alpha_S(M_Z)$ and the PDF parameters
- The difference between the PDF parameters obtained in this way compared to the result obtained using a fixed value of $\alpha_S(M_Z)$ is negligible, but the uncertainties are a bit larger.
- The value of $\alpha_S(M_Z)$ extracted from this fit is:

$$\alpha_S(M_Z) = 0.1166 \pm 0.0008(\text{stat.}) \pm 0.0032(\text{corr.}) \pm 0.0036(\text{norm.}) \pm 0.0018(\text{model})$$



Summary of α_S measurements at ZEUS



2000-2002 HERA Upgrade.

- *All HERA results so far shown from HERA I running period 1993-2000 $\approx 120 \text{ pb}^{-1}$ data (as taken by ZEUS).*
- *From 2000-2002 HERA underwent a luminosity upgrade and aims to provide $\approx 100 \text{ pb}^{-1}$ taken by ZEUS/H1 per year.*
- *ZEUS took 41 pb^{-1} in 2003-4*
- *In addition HERA can now provide polarised leptons.*
- *ZEUs and H1 have undergone their own upgrades.*
- *ZEUS:*
 - *New silicon vertexing detector.*
 - *New Straw tube tracker in the forward region.*
 - *New (supplementary) luminosity monitor.*
- *H1:*
 - *New Trigger.*
 - *New tracking detectors.*

What's new at HERA II?

- *Polarised DIS measurements:*
 - *Important test of electroweak physics.*
 - *Early results are promising.*
- *Heavy Flavour (c, b) physics:*
 - *New trackers at ZEUS improve heavy meson tagging.*
 - *Better tracking based triggers available.*
- *Improved exotic physics searches:*
 - *Extra lumi helps probability of discovery , or at least improvement of limits.*
 - *Leptoquark, single top via FCNC two of the main exotic physics searches.*

Deep Inelastic Scattering with Longitudinally Polarised Leptons

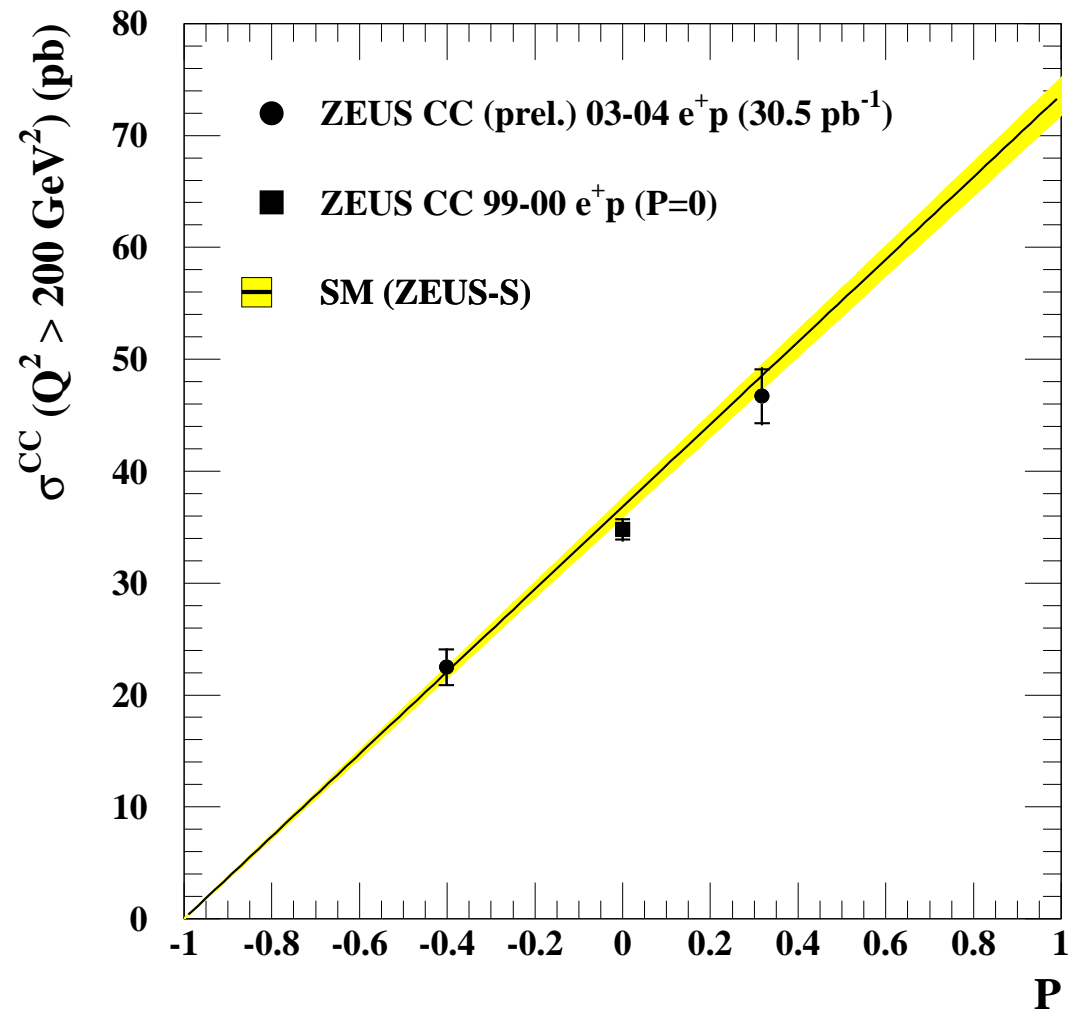
- *Beams at HERA have natural transverse momentum.*
- *Rotator magnets rotate the polarisation into the longitudinal direction.*
- *Mean Polarisation values of -40% and $+31.8\%$ have been produced in 2003-4 HERA II running.*
- *Polarisation affects the CC and NC cross section, CC dependence is simple:*

$$\frac{d^2\sigma_{(\text{CC Polarised DIS } e^+p)}}{dx dQ^2} = (1 + \mathcal{P}) \frac{d^2\sigma_{(\text{CC unpolarised DIS } e^+)}}{dx dQ^2}$$

- *NC dependence weaker and more complicated:*

$$\frac{d^2\sigma_{(\text{NC Polarised DIS } e^+p)}}{dx dQ^2} = \frac{2\pi\alpha^2}{xQ^2} [H_0^+ + \mathcal{P}H_{\mathcal{P}}^+]$$

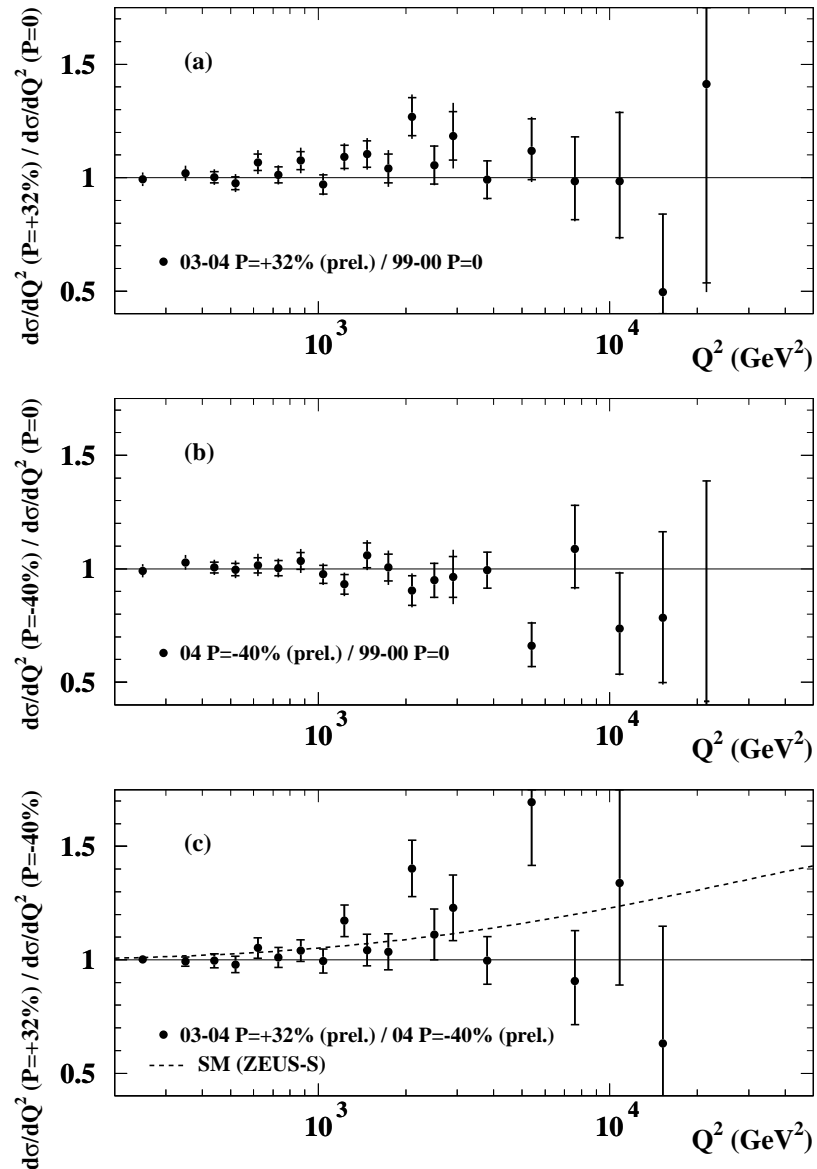
H_0^+ is our usual unpolarised e^+p structure function terms. $H_{\mathcal{P}}^+$ is the same but using the polarised structure functions.

CC DIS with Polarised Positrons**ZEUS**

- *The first measurement of the polarised cross sections.*
- *Good agreement with the standard Model*

NC DIS with Polarised Positrons

ZEUS



- *The first measurement of the polarised cross sections.*
- *Good agreement with the standard Model.*
- *Polarised effect is not conclusively observed.*

Lecture IV : Summary

- *Many measurements of α_S are made to pin down this fundamental parameter of QCD.*
- *To avoid sensitivity to PDFs cross section ratios are used.*
- *A simultaneous fit of α_S and PDFs can yield excellent results*
- *There are many consistent measurements of α_S*
- *HERA II is now running:*
 - *Polarisation effect on Charged Current observed.*
 - *No confirmation of polarisation effect on NC.*
- *Much more physics still to come from HERA...*